Eur. Phys. J. D **26**, 141–146 (2003)
DOI: 10.1140/epjd/e2003-00213-7

THE EUROPEAN PHYSICAL JOURNAL D

Triple differential cross-sections of Ne ($2s^2$) in coplanar to perpendicular plane geometry

L.Q. Chen, Y. Khajuria, X.J. Chen[a], and K.Z. Xu

Open Laboratory of Bond Selective Chemistry, Department of Modern Physics, University of Science and Technology of China, Hefei, Anhui 230027, P.R. China

Received 7 November 2001 / Received in final form 16 July 2002
Published online 22 July 2003 –

Abstract. The distorted wave Born approximation (DWBA) with the spin averaged static exchange potential has been used to calculate the triple differential cross-sections (TDCSs) for Ne ($2s^2$) ionization by electron impact in coplanar to perpendicular plane symmetric geometry at 110.5 eV incident electron energy. The present theoretical results at gun angles $\Psi = 0°$ (coplanar symmetric geometry) and $\Psi = 90°$ (perpendicular plane geometry) are in satisfactory agreement with the available experimental data. A deep interference minimum appears in the TDCS in the coplanar symmetric geometry and a strong peak at scattering angle $\xi = 90°$ caused by the single collision mechanism has been observed in the perpendicular plane geometry. The TDCSs at the gun angles $\Psi = 30°$, and $\Psi = 60°$ are predicted.

PACS. 34.80.Gs Molecular excitation and ionization by electron impact – 34.80.Dp Atomic excitation and ionization by electron impact

1 Introduction

The inner shell ionization of atoms, ions and molecules by electron impact is important in electron momentum spectroscopy, Auger electron spectroscopy, electron energy loss spectroscopy and other fields. The first measurement of (e, $2e$) TDCS for inner shell ionization of Ar ($2p$) was made by Lahmam-Bennani *et al.* [1], which employed incident electron energy of 8399 eV and ejected electron energy of 150 eV. The scattering angles were chosen as 1°, 1.25°, 4° and 7°. They found a strong recoil peak at all scattering angles, even stronger than binary one at small scattering angles. Measurement on Ar ($2p$) was also made by Stefani *et al.* [2] for the incident energy of 8031.5 eV and ejected electron energy of 7 eV. The scattering angle was kept at 1.5°. They observed a large binary peak in the direction of momentum transfer and a recoil peak opposite to it. Measurements on Ar ($2p$) have been extended to the lower energies of 2–3 keV as well as to the larger momentum transfers (Bickert and Hink [3], Bickert *et al.* [4–6], Bickert [7]). Lohmann and Cavanagh [8] performed the experiment on Ar ($2p$) at even lower energy of 1249 eV. The characteristic feature of the TDCSs measured in the above mentioned inner-shell ionization studies is the dominant recoil peak. The cylindrical symmetry of the TDCSs about the direction of the momentum transfer, which was observed at high incident energies, was not observed at low incident energies. The deviations from the cylindrical symmetry were exhibited by Lohmann and Cavanagh [8]: both binary and recoil peaks were shifted towards larger angles.

The plane wave Born and impulse approximations were used in most of the calculations of the inner shell ionization cross-sections. These were completely inadequate to describe the Ar ($2p$) experiments, as the plane wave approximations only considered incident electron-target electron interaction. For example, almost no recoil lobe was obtained, which was very large in the experiments. Brothers and Bonham [9] employed the frozen-core factorized plane-wave first-Born approximation to calculate the TDCS of Ar ($2p$). The ejected electron was described by a Coulomb wavefunction and the target ground state was described by Clementi-type analytic Hartree-Fock one-electron wavefunction. The final state wavefunction was made both non-orthogonal and orthogonal to the initial state wavefunction, and the effective charge seen by the ejected electron was adjusted to match the theoretical TDCS with the experimental one at the maximum of the binary lobe. Brothers and Bonham concluded that their description of the ejected electron wavefunction was inadequate, because the distortion of the ejected electron wave was not explicitly involved. Grum-Grzhimailo [10] reported the results using first Born approximation (FBA). The distortion of the ejected electron wavefunction was taken into account more accurately by using the Hartree-Slater wavefunctions for the discrete state and the continuum. This theory reproduced better the recoil peak, still with a large discrepancy in the binary lobe at small

[a] e-mail: xjun@ustc.edu.cn

scattering angles. This discrepancy could be attributed to the lack of accuracy of Hartree-Slater model.

Botero and Macek [11] calculated the TDCS of C ($1s^2$) using Coulomb-Born approximation. They neglected the final state correlation between scattered and ejected electrons. Nath *et al.* [12] included this correlation by choosing the final state as the product of three Coulomb wave functions of Brauner, Briggs, and Klar (BBK) [13]. Zhang *et al.* [14] nicely explained the measurements made by Bickert [7] by using the distorted wave Born approximation (DWBA).

Recently Murray and Read [15] performed an experiment on the Ne ($2s^2$) at gun angles of $\Psi = 0°$, 42°, 90°. The incident electron energy was 110.5 eV and the two outgoing electrons were detected with equal energy of 31 eV. For $\Psi = 42°$, they compared their experimental result with the theoretical result of Rasch *et al.* [16]. Rasch *et al.* [16] used the DWBA including the post-collisional interaction (PCI) in the final state. The distorted-wave for the incident electron was generated in the static-exchange potential of the atom and the distorted-waves for the outgoing electrons were each generated in the static-exchange potential of the ion.

In the present paper, the theoretical TDCSs for electron impact ionization of Ne ($2s^2$) are calculated in the DWBA for the incident electron energy of 110.5 eV in symmetric geometry at gun angles $\Psi = 0°$ (coplanar geometry), 30°, 42°, 60°, 90° (perpendicular plane geometry). The present results are compared with the experimental results of Murray and Read [15] and the theoretical result of Rasch *et al.* [16].

2 Theory

The TDCS is the measurement of the probability of the $(e,\ 2e)$ reaction that an incident electron of energy E_0 and momentum k_0 colliding with the target produces two electrons (ejected and scattered) with energies E_1, E_2 and momenta k_1, k_2 satisfying the energy relation:

$$E_0 = E_1 + E_2 + \varepsilon \tag{1}$$

where ε is the ionization potential of the target.

The triple differential cross-section is given in atomic units as:

$$\frac{\mathrm{d}^3\sigma}{\mathrm{d}\Omega_1\mathrm{d}\Omega_2\mathrm{d}E_1} = M_{ee}(2\pi)^4\frac{k_1k_2}{k_0}\sum_{\mathrm{av}}\left(|f|^2 + |g|^2 - \mathrm{Re}(f^*g)\right) \tag{2}$$

where

$$f \equiv \left\langle \chi^{(-)}(k_1, r_1)\chi^{(-)}(k_2, r_2)|V_{12}|\chi^{(+)}(k_0, r_1)\psi_{nl}\right\rangle, \tag{3a}$$

$$g \equiv \left\langle \chi^{(-)}(k_1, r_2)\chi^{(-)}(k_2, r_1)|V_{12}|\chi^{(+)}(k_0, r_1)\psi_{nl}\right\rangle, \tag{3b}$$

$\sum_{\mathrm{av}}$ represents sum over final and average over initial magnetic and spin degeneracy. r_1 and r_2 are the coordinates of the outgoing electrons. The Gamov factor M_{ee}, same as the Gamov factor of Rasch *et al.* [16], takes into account the PCI. $V_{12} = 1/|r_1 - r_2|$ is the interaction potential between the incident and target electrons responsible for the ionization. ψ_{nl} represents the nl orbital of the target atom. $\chi^{(+)}$ is the distorted wave for the incident electron generated in the equivalent local ground state potential for the incident electron and $\chi^{(-)}$ denote the distorted waves for the outgoing electrons generated in the equivalent local ground state potential of outgoing electrons. $\chi^{(+)}$ and $\chi^{(-)}$ are both orthogonalized to ψ_{nl}. The partial wave expansion for the distorted waves and the multipole expansion for the interaction potential V_{12} have been considered in detail by McCarthy [17]. The spin averaged static exchange potential with the exchange potential taken in the equivalent local approximation [18] is given as

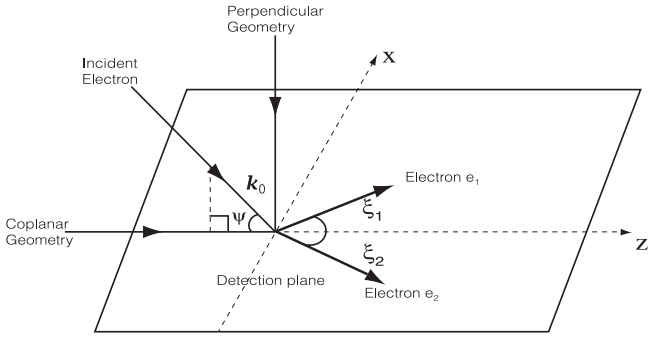

Fig. 1. The $(e,\ 2e)$ geometry employed in present calculation.

$$V_E(r) = 0.5\left(E_0 + V_D(r) - \left\{[E_0 + V_D(r)]^2 - 2\pi\rho(r)\right\}^{\frac{1}{2}}\right) \tag{4}$$

where $\rho(r)$ is the electron density. The direct distorting potential $V_D(r)$ for the incident electron is obtained from the target-atom radial orbitals $u_{nl}(r)$ [17] as

$$V_D(r) = \sum_{nl} N_{nl}\int \mathrm{d}r'[u_{nl}(r')]^2/r_\rangle, \tag{5}$$

where $r_\rangle$ is the greater of r and r', N_{nl} is the number of electrons in each orbital nl. For the outgoing electrons, direct distorting potential $V_D(r)$ is obtained from the ion radial orbitals. The equivalent local ground state potential V_{00} (*i.e.* distorting potential) is the sum of exchange and direct potentials:

$$V_{00} = V_D(r) + V_E(r). \tag{6}$$

The orbital ψ_{nl} in equation (3) is taken from the Hartree-Fock wavefunction given by Clementi and Roetti [19]. The parameters such as the maximum orbital angular momenta in the partial wave expansions (55 partial waves for the incident electron, 50 partial waves for slower outgoing electron and 45 partial waves for fast outgoing electron) and mesh size of the integration have been optimized in order to satisfactorily converge the cross-sections.

The geometry of the process, similar to [15], is shown in Figure 1. The two outgoing electrons having momenta k_1 and k_2 define the detection plane. The gun angle Ψ is defined as the angle between the detection plane and the

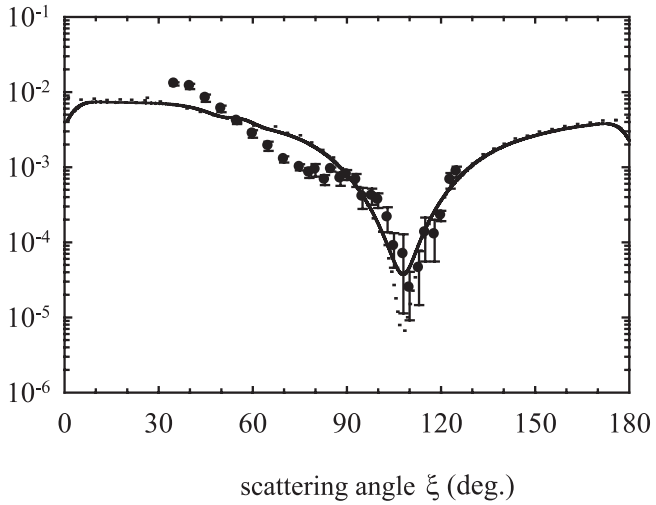

Fig. 2. TDCSs for the Ne ($2s^2$) ionization at 110.5 eV incident energy in the coplanar symmetric geometry. Dotted line represents the present unconvoluted results, solid line represents the convoluted results and dots denote the experimental data from [15].

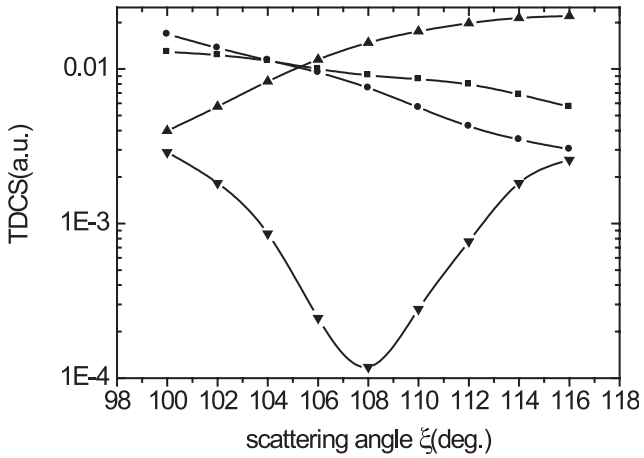

Fig. 3. TDCSs at 110.5 eV incident electron energy in coplanar symmetric geometry in the region of the deep minimum. Calculations with different distorting potentials are presented: (—■—) the distorting potential without electron-nucleus interaction, (—●—) the distorting potential without electron-passive electron interaction, (—▲—) the distorting potential without electron-nucleus and electron-passive electron interactions and (—▼—) the full distorting potential.

direction of the incident electron beam. The scattering angles ξ_1 and ξ_2 are the angles between the momenta of outgoing electrons and the projection of the incident electron momentum onto the detection plane. For symmetric geometry $\xi_1 = \xi_2 = \xi$, $|k_1| = |k_2|$. For coplanar geometry $\Psi = 0°$, while for perpendicular plane geometry $\Psi = 90°$.

3 Results

The present results at $\Psi = 0°$, $30°$, $42°$, $60°$, $90°$ are shown in Figures 2–5, 8, 9. The results at $\Psi = 0°$, $42°$, $90°$ are convoluted with Gaussian angular profile of $\pm 4.5°$ and shown along with the experimental results of Murray and Read [15]. According to [20–22] there exists a common point in the cross-sections at $\xi = 90°$, so the present theoretical TDCSs at $\Psi = 0°$ and $\Psi = 90°$ have been normalized at this point. At all gun angles, the magnitude of the TDCSs (before the normalization) with the PCI taken into account is smaller than without including the PCI.

The theoretical results at $\Psi = 0°$ are shown in Figure 2. After the normalization the TDCSs with and without including the PCI are indistinguishable. They are in good agreement with the experimental data between $\xi = 90°$ and $\xi = 130°$, but some discrepancies remain at smaller scattering angles. There exists a deep minimum in the cross-section curve at $\xi = 110°$. The position and the relative magnitude of this minimum are in satisfactory agreement with the experimental data. The minimum in the theoretical curve becomes shallower after the convolution and matches the experimental results better. In case of e^-He, Murray and Read [21] have explained that the minimum in the TDCS is due to the almost complete cancellation of all contributing scattering amplitudes. Furthermore, Khajuria and Tripathi [20] have shown for He that the deep minimum is due to the strong interference effect between the incoming and outgoing wavefunctions and disappears when switching off any component of the distorting potential (the equivalent local ground state potential). The TDCSs in the region of the deep minimum between $\xi = 100°$ and $\xi = 116°$ are shown in Figure 3. The TDCSs are calculated by switching off one of the following interactions from the distorting potential $V_{00} = V_D(r) + V_E(r)$ at a time: (i) electron-nucleus interaction, (ii) electron-passive electrons interaction (passive electrons are residual electrons of the target except the ionized electron), (iii) both electron-nucleus interaction and electron-passive interaction. It can be seen from Figure 3 that only the TDCS obtained with the full distorting potential V_{00} gives the minimum, whereas switching off any of the components in the distorting potential V_{00} smoothes the cross-section curve. It clearly indicates that in case of Ne ($2s^2$) the minimum is due to the strong interference between the different scattering wavefunctions constituting the total scattering wavefunction.

The theoretical TDCSs for the gun angle of $\Psi = 42°$ shown in Figure 4 are normalized at $\xi = 35°$ similar to Murray and Read [15]. There is a little difference between the shape of the TDCSs with and without the PCI. The result with the PCI is better than without it compared with the experiment, so only the convoluted curve with the PCI included is shown. There are two minima at $\xi = 50°$ and $\xi = 100°$ in our theoretical curves. Also two minima occur at $\xi = 54°$ and $\xi = 115°$ in experimental TDCS of Murray and Read [15] and at $\xi = 51°$ and $\xi = 105°$ in convoluted theoretical TDCS of Rasch *et al.* [16]. The positions of the first minimum for the three results are in agreement with each other, while the positions of the second minimum differ a little.

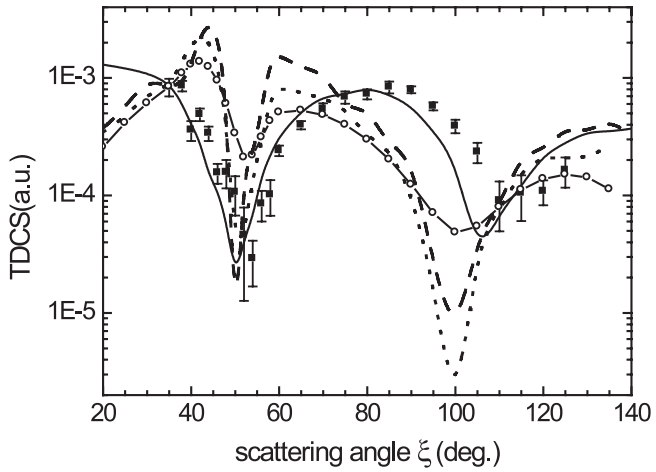

Fig. 4. TDCSs for the Ne ($2s^2$) ionization at 110.5 eV incident energy for gun angle $\Psi = 42°$. Dashed line represents the unconvoluted result with the PCI. The dotted line represents the unconvoluted result without the PCI. (—o—) represents the convoluted result with the PCI. The solid line represents the convoluted theoretical result of Rasch *et al.* [16]. Experimental data are taken from [15].

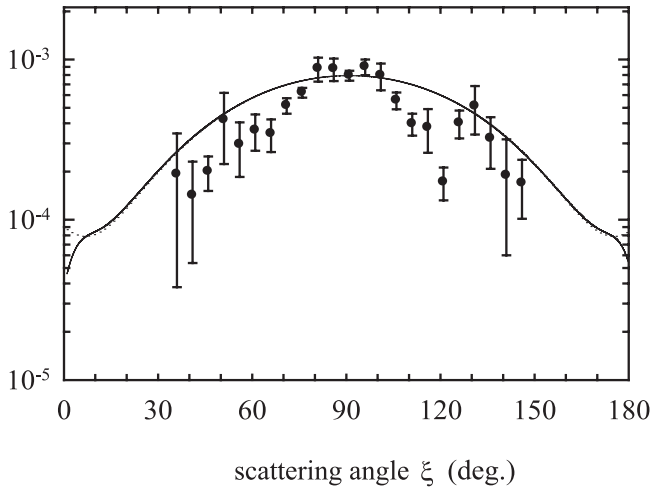

Fig. 5. Same as Figure 2, but for perpendicular plane geometry.

The TDCS at the gun angle of $\Psi = 90°$ is shown in Figure 5. The TDCSs with and without the PCI included are indistinguishable after the normalization. Our theoretical TDCS shows a broad maximum at $\xi = 90°$, while the experimental data show a peak at $\xi = 90°$ and two side peaks at $\xi = 50°$ and $\xi = 130°$. The peak at $\xi = 50°$ is equivalent to the peak at $\xi = 130°$, because the TDCS is symmetric about $\xi = 90°$ in the perpendicular plane geometry. Zhang *et al.* [23] have reported two peaks in the TDCS of He at $\xi = 45°$ and $\xi = 90°$ at perpendicular plane geometry. The peak at $\xi = 45°$, as pointed out by Byron *et al.* [24], is caused by the double scattering mechanism and the peak at $\xi = 90°$ is due to the single scattering mechanism. Within the single scattering mechanism, when the incident electron with the momentum k_0 collides with the target electron with the momentum $p = p_{\|} + p_{\perp}$ (Fig. 6), $p_{\perp} + k_0 = 0$ and $p_{\|} = k_1 + k_2$, provided the outgoing electrons emerge in the plane perpendicular to the incident electron beam. For s-electron, like in He ($1s^2$) and Ne ($2s^2$), the momentum distribution (spherically averaged momentum density) peaks at $p = 0$ (p is the absolute value of the electron momentum) and decreases rapidly as p increases as shown in Figure 7. Thus the most likely value of $p_{\|}$ is zero (since $p^2 = p_{\|}^2 + k_0^2$) and the outgoing electrons will be ejected most probably in opposite directions ($\xi = 90°$) in the perpendicular plane. For the double collision mechanism, first the incident electron elastically scatters from the target (essentially from nucleus) through 90°, then by the second momentum and energy conserving collision the target electron is ionized with both of the electrons emerging in the perpendicular plane and at 90° to each other. Zhang *et al.* [23] have calculated the TDCS of He in the perpendicular plane geometry at different incident electron energies. They have noticed that for He at sufficient low incident electron energies the peak at $\xi = 90°$ dominates over the peak at $\xi = 45°$, but with increasing of the incident electron energy, the peak at $\xi = 45°$ gradually dominates over the peak at $\xi = 90°$.

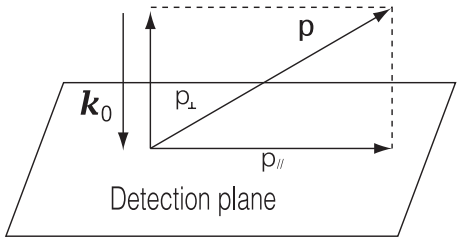

Fig. 6. Kinematic scheme for single collision mechanism.

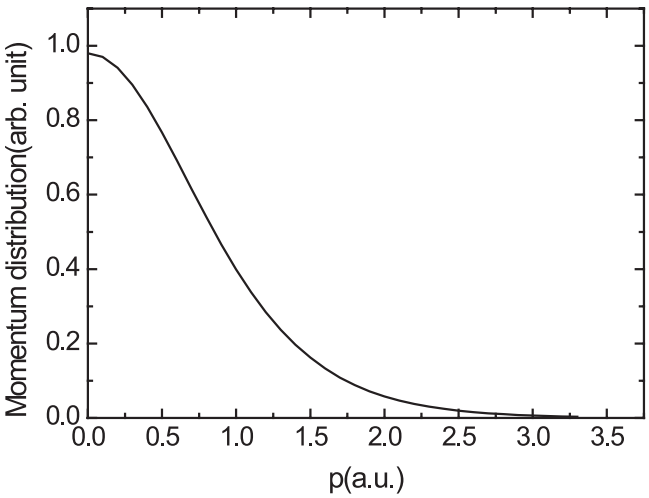

Fig. 7. Momentum distribution of the 2s-electron in Ne.

According to the above discussion, the peak at $\xi = 90°$ observed by Murray and Read [15] is due to the single scattering mechanism and the two side peaks at $\xi = 50°$ and $\xi = 130°$ are due to the double scattering mechanism. The present calculation only reproduces the peak at $\xi = 90°$. The possible reason is that the interaction between incident electron and nucleus is not included in the interaction

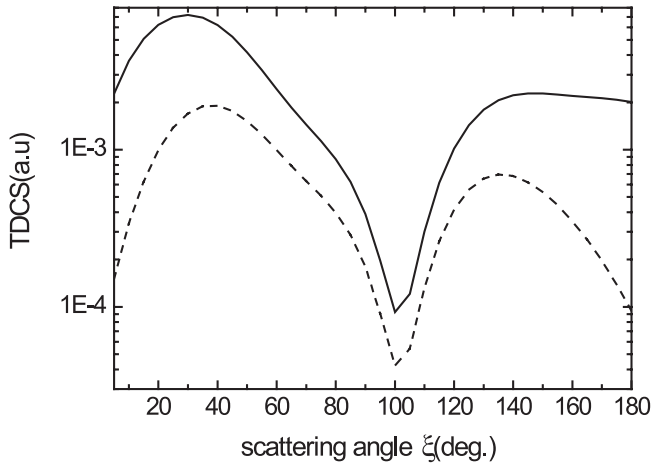

Fig. 8. Our calculated triple differential cross-sections of Ne ($2s^2$) at 110.5 eV incident energy at $\Psi = 30°$. Dotted line represents the result with the PCI and solid line represents the result without the PCI.

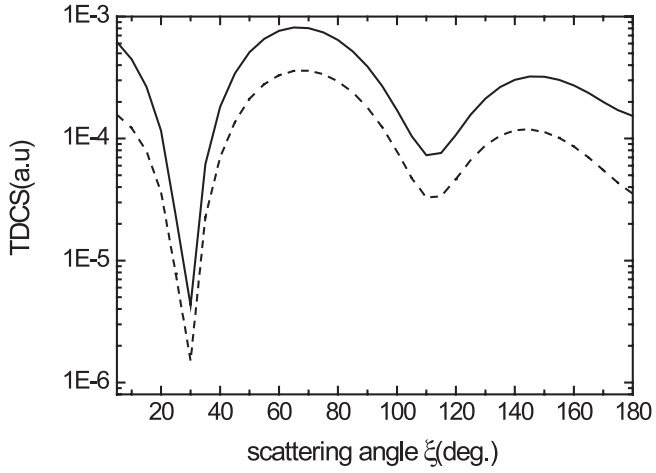

Fig. 9. Same as Figure 8, but for $\Psi = 60°$.

potential V_{12} in equations (3a, 3b), but for inner shell ionization of the heavy atom, especially in double scattering process, the interaction potential between incident electron and nucleus is very important since the ionization process takes place relatively close to the nucleus.

Calculated TDCSs for the gun angles of $\Psi = 30°$ and $\Psi = 60°$ are shown in Figures 8 and 9. Including the PCI makes the cross-sections substantially smaller. There is a little difference between the shapes of both TDCSs at $\Psi = 30°$, while the shape of both TDCSs at $\Psi = 60°$ is almost the same. There is one minimum at $\xi = 100°$ for $\Psi = 30°$ and two minima at $\xi = 30°$ and $\xi = 115°$ for $\Psi = 60°$. The minimum at $\xi = 30°$ is deeper than the minimum at $\xi = 115°$.

Finally, we come to the following conclusions:

(i) DWBA with the spin averaged static exchange potential is very successful in explaining the deep minimum in (e, $2e$) TDCS of Ne ($2s^2$) in coplanar symmetric geometry;

(ii) the above version of DWBA is successful in predicting the first minimum of the TDCS for the gun angle of $\Psi = 42°$, but shows some discrepancies with experimental data in predicting the position of the second minimum. The reasons of quantitative difference between our results and the results of Rasch *et al.* [16], who used the similar DWBA methods, remain unclear;

(iii) the present theory is successful in reproducing the peak at $\xi = 90°$ in perpendicular geometry caused by the single scattering mechanism, but fails to predict the peaks at $\xi = 50°$ and $\xi = 130°$ caused by double collision mechanism [23]. The possible reason is that the interaction between incident electron and nucleus was not included in the interaction potential V_{12} in equations (3a, 3b);

(iv) the present calculations predict one minimum in the TDCS for the gun angle $\Psi = 30°$ and two minima for the gun angle $\Psi = 60°$;

(v) at all gun angles, the positions of the minima of the TDCSs are almost unaffected by inclusion of the PCI, while the value of the TDCS decreases. The shape of the TDCSs with and without the PCI is almost similar at all gun angles except at $\Psi = 30°$ and $\Psi = 42°$;

(vi) further studies are needed to explain remaining discrepancies between theoretical and experimental TDCSs.

Financial support for this research were provided by the National Natural Science Foundation of China (Grant Nos: 19634040 and 19974040). One of the authors, YK, is grateful to the Chinese Academy of Science (CAS) for providing the necessary grants. We would like to thank Prof. J. Chen and Mr. X. Shan for valuable discussions.

References

1. A. Lahmam-Bennani, H.F. Wellenstein, A. Duguet, A. Daoud, Phys. Rev. A **30**, 1511 (1984)
2. G. Stefani, L. Avaldi, A. Lahmam-Bennani, A. Duguet, J. Phys. B: At. Mol. Opt. Phys. **19**, 3787 (1986)
3. P. Bickert, W. Hink, *2nd Eur. Conf. on (e, 2e) Collisions and Related Problems*, Kaiserslautern, edited by H. Ehrhardt, Invited Papers and Progress Reports, p. 38, 1989
4. P. Bickert, S. Schönberger, W. Hink, *3rd Eur. Conf. on (e, 2e) Collisions and Related Problems*, Rome, edited by G. Stefani, Invited Papers and Progress Reports, p. 55, 1990
5. P. Bickert, W. Hink, C.D. Cappello, A. Lahmam-Bennani, J. Phys. B: At. Mol. Opt. Phys. **24**, 4603 (1991)
6. P. Bickert, W. Hink, S. Schönberger, *Proc. 17th Int. Conf. on Physics of Electronic and Atomic Collisions*, Brisbane, edited by I.E. McCarthy, W.R. MacGillivray, M.C. Standage, Abstracts p. 180, 1991
7. P. Bickert, thesis, university of Wurzburg, Germany, 1991
8. B. Lohmann, S. Cavanagh, Can. J. Phys. **74**, 743 (1996)
9. M.J. Brothers, R.A. Bonham, J. Phys. B: At. Mol. Opt. Phys. **19**, 3801 (1986)

10. A.N. Grum-Grzhimailo, J. Phys. B: At. Mol. Opt. Phys. **18**, L695 (1985)
11. J. Botero, J.H. Macek, Phys. Rev. A **45**, 154 (1992)
12. B. Nath, R. Biswas, C. Sinha, Z. Phys. D **42**, 157 (1997)
13. M. Brauner, J.S. Briggs, H. Klar, J. Phys. B: At. Mol. Opt. Phys. **22**, 2265 (1989)
14. X. Zhang, C.T. Whelan, H.R.J. Walters, R.J. Allan, P. Bickert, W. Hink, S. Schönberger, J. Phys. B: At. Mol. Opt. Phys. **25**, 4325 (1992)
15. A.J. Murray, F.H. Read, Phys. Rev. A **63**, 012714 (2000)
16. J. Rasch, C.T. Whelan, R.J. Allan, S.P. Lucey, H.R.J. Walters, Phys. Rev. A **56**, 1379 (1997)
17. I.E. McCarthy, Aust. J. Phys. **48**, 1 (1995)
18. J.B. Furness, I.E. McCarthy, J. Phys. B: At. Mol. Opt. Phys. **6**, 2280 (1973)
19. E. Clementi, C. Roetti, At. Data Nucl. Data Tables **14**, 177 (1974)
20. Y. Khajuria, D.N. Tripathi, J. Phys. B: At. Mol. Opt. Phys. **31**, 2359 (1998)
21. A.J. Murray, F.H. Read, J. Phys. B: At. Mol. Opt. Phys. **26**, L359 (1993)
22. A.J. Murray, (e, $2e$) *and Related Processes*, edited by C.T. Whelan, H.R.J. Walters, A.L. Bennani, H. Ehrhardt (Kluwer Academic publisher, 1993), p. 327
23. X. Zhang, C.T. Whelan, H.R.J. Walters, J. Phys. B: At. Mol. Opt. Phys. **23**, L173 (1990)
24. F.W. Byron Jr, C.J. Joachain, B. Piraux, J. Phys. B: At. Mol. Opt. Phys. **16**, L769 (1983)